HHS Public Access

Author manuscript

AIDS. Author manuscript; available in PMC 2016 August 24.

Published in final edited form as:

AIDS. 2015 August 24; 29(13): 1597–1606. doi:10.1097/QAD.0000000000000702.

Lack of viral control and development of cART escape mutations in macaques after bone marrow transplantation

Christopher W. PETERSON[1,*], **Kevin G. HAWORTH**[1,*], **Patricia POLACINO**[2,3], **Meei-Li HUANG**[5], **Craig SYKES**[4], **Willimark M. OBENZA**[1], **Andrea C. REPETTO**[5], **Angela KASHUBA**[4], **Roger BUMGARNER**[2], **Stephen C. DeROSA**[5], **Ann E. WOOLFREY**[1,2], **Keith R. JEROME**[5], **James I. MULLINS**[2], **Shiu-Lok HU**[2,3], and **Hans-Peter KIEM**[1,2]

[1]Clinical Research Division, Fred Hutchinson Cancer Research Center, Seattle, WA, 98109, USA

[2]University of Washington, Seattle, WA, 98195, USA

[3]Washington National Primate Research Center, Seattle, WA, 98121, USA

[4]Division of Pharmacotherapy and Experimental Therapeutics, University of North Carolina, Chapel Hill, NC, 27599, USA

[5]Vaccine and Infectious Disease Division, Fred Hutchinson Cancer Research Center, Seattle, WA 98109, USA

Abstract

Objective—We have previously demonstrated robust control of simian/human immunodeficiency virus (SHIV1157-ipd3N4) viremia following administration of combination antiretroviral therapy (cART) in pigtailed macaques. Here, we sought to determine the safety of hematopoietic stem cell transplantation (HSCT) in cART-suppressed and unsuppressed animals.

Design—We compared disease progression in animals challenged with SHIV 100 days post-transplant (PT), to controls that underwent transplant following SHIV challenge and stable, cART-dependent viral suppression.

Methods—SHIV viral load, combination antiretroviral therapy (cART) levels, and anti-SHIV antibodies were measured longitudinally from plasma/serum from each animal. Flow cytometry

Corresponding Author: Hans-Peter Kiem, MD, Fred Hutchinson Cancer, Research Center, 1100 Fairview Ave N, Mail Stop D1-100, PO Box 19024, Seattle, WA 98109-1024, Phone: 206-667-4425, Fax: 206-667-6124, hkiem@fhcrc.org.

*Equal Contribution

Authors' contributions: HPK is the principal investigator of the study. CWP and KGH designed, conducted, and coordinated the experiments. CWP and PP coordinated the animal experiments. MLH conducted the SHIV DNA measurements. CS, JIM, and AK designed and conducted the cART measurement experiments. WMO, ACR, and SCD conducted the flow cytometry experiments. RB and JIM designed and conducted the viral sequencing experiments. AEW, KRJ, JIM, and SLH contributed substantially to the study conception and design, and critically reviewed the manuscript. We thank Helen Crawford for help in preparing this manuscript, and Lisa Frenkel for helpful discussions. We also thank Veronica Nelson, Erica Curry, and Kelvin Sze for excellent support in our pigtailed macaque studies, Larry Stensland for total SHIV DNA measurements, Michael Watling for conducting sequencing assays, Baoping Tian and Heather Mack for technical assistance with T-cell phenotyping experiments, and Leon Flannery and Joel Ahrens for conducting GI biopsy procedures. The SHIV1157-ipd3N4 inoculum used in these studies was kindly provided by Ruth Ruprecht. Tenofovir and Emtricitabine were kindly provided by Gilead Sciences. Raltegravir was kindly provided by Merck. H.-P. Kiem is a Markey Molecular Medicine Investigator and received support as the inaugural recipient of the José Carreras/E. Donnall Thomas Endowed Chair for Cancer Research.

was used to assess T-cell subset frequencies in peripheral blood and gastrointestinal tract (GI). Deep sequencing was used to identify cART resistance mutations.

Results—In control animals, virus challenge induced transient peak viremia, viral set point, and durable suppression by cART. Subsequent HSCT was not associated with adverse events in these animals. PT animals were challenged during acute recovery following HSCT, and displayed sustained peak viremia and cART resistance. Although PT animals had comparable plasma levels of antiretroviral drugs and showed no evidence of enhanced infection of myeloid subsets in the periphery, they exhibited a drastic reduction in virus-specific antibody production and decreased T-cell counts.

Conclusions—These results suggest that virus challenge prior to complete transplant recovery impairs viral control and may promote drug resistance. These findings may also have implications for scheduled treatment interruption (STI) studies in patients on cART during post-HSCT recovery: premature STI could similarly result in lack of viral control and cART resistance.

Keywords

HIV/AIDS; hematopoietic stem cell transplant; gene therapy

Introduction

Hematopoietic stem cell transplantation (HSCT) remains the only clinically exemplified route to functional cure/remission of HIV-1 infection [1–3]. The “Berlin Patient”, an HIV+ patient diagnosed with acute myeloid leukemia (AML), was transplanted with allogeneic, HLA-matched, CCR5Δ32/Δ32 cells in February of 2007, and was removed from his combination antiretroviral therapy (cART) regimen concurrently. Following AML relapse and a second transplant in March of 2008, CD4+ T-cell counts recovered, and he remains free of detectable replication-competent virus, in the absence of cART, over 8 years later [4]. More recently, two lymphoma patients in Boston received allogeneic transplants with CCR5wt/wt cells. After hematopoietic recovery and extensive monitoring on cART, during which time HIV-1 was undetectable by multiple ultrasensitive assays, both patients were removed from cART, but continued on immunosuppressive therapy [5]. Viral rebound was observed within 12–32 weeks, and drug-resistant plasma viremia was encountered following re-initiation of cART in one of the two patients, necessitating transition to a new cART regimen [6]. The findings in the Berlin and Boston patients strongly suggest that cART disruption while still immunosuppressed is associated with viral rebound and the potential for resistance.

We have developed a model of HSCT in the pigtailed macaque, *M. nemestrina* [7–9]. Recently, we adapted our system to model gene therapy-mediated cure/remission of HIV-1 infection using the wealth of knowledge regarding SIV and SHIV infection in nonhuman primate species including *M. nemestrina* ([10–13]. In this study we asked whether the immune response to SHIV challenge in transplanted animals was comparable to that in untransplanted controls.

Materials and Methods

Animal welfare statement

This study was carried out in strict accordance with the recommendations in the Guide for the Care and Use of Laboratory Animals of the National Institutes of Health. The protocol was approved by the Institutional Animal Care and Use Committees of the Fred Hutchinson Cancer Research Center and University of Washington.

Animals

Seven healthy male juvenile pigtailed macaques (*M. nemestrina*) were housed at the Washington National Primate Research Center. Animals Z09087, Z09106, and Z09192 (Group I) and Z09144 and Z08214 (Group II) were challenged with 9500 TCID50 SHIV-1157ipd3N4 intravenously, and initiated cART 6 months post-SHIV challenge as previously described [11]. Approximately 1 year following infection, CD34+ hematopoietic stem cells from Group II animals, which were collected prior to SHIV challenge and cryopreserved [14], were thawed and transduced with a BFP-expressing lentiviral vector. BFP fluorescence was not analyzed for the purposes of this study. Cells were infused into the autologous animal following administration of myeloablative total body irradiation (TBI), consistent with our established protocols [14]. Animals A11202 and A11205 (Group III) were transplanted with a non-optimized CCR5 targeting protocol that generated physiologically irrelevant to undetectable levels of CCR5 gene disruption. At 100 days post-transplant, these animals were also challenged with SHIV-1157ipd3N4. Due to declining health as described below, these animals initiated cART roughly four months earlier than Groups I–II.

Please see Supplementary Methods and Materials for Further Information

Results

Development of cART resistance in post-transplant animals

The different experimental groups used in this study are outlined in Figure 1A. We compared three animals that were challenged with SHIV, but did not undergo transplant (“Group I: No transplant”), two animals that were transplanted subsequent to SHIV challenge (“Group II: SHIV-transplant”), and two animals that were challenged with SHIV post-transplant (PT; “Group III: transplant-SHIV”). All seven animals were challenged with 9500 TCID50 of the CCR5-tropic env-SHIV, SHIV1157-ipd3N4 intravenously, and received a 3-drug cART regimen following SHIV challenge. As shown in Figures 1B–1C, Group I and II animals displayed ranges of peak viral load and viral set points that were consistent with previous observations made by our lab and others [11, 15, 16]. In all Group I and II animals, 3-drug cART initiated at 25 weeks durably suppressed plasma viremia, with occasional viral blips, to the limit of detection of our assay (30 copies/mL). Group II animals remained durably suppressed during hematopoietic stem cell transplant (Figure 1C). By contrast, Group III animals exhibited sustained peak viremia through 10 weeks, with associated thrombocytopenia and low hematocrit (Figure 1D and data not shown) necessitating an earlier initiation of cART (Groups I–II: week 25–27; Group III: week 9–

10). Interestingly, neither Group III animal was effectively suppressed by cART; although plasma viremia declined, it remained 2–4 logs above the limit of detection (Figure 1D). These results suggest that immunosuppressed animals undergo a more severe course of acute infection relative to controls, including sustained viremia and resistance to a previously validated cART regimen [11].

Resistance mutations in SHIV-C map to cART target genes Pol and RT

We hypothesized that cART resistance in Group III animals could be due to development of cART resistance mutations. We therefore employed a deep sequencing approach to monitor viral evolution in these animals. Total RNA was isolated from plasma from Groups I, II, and III at multiple time points following SHIV challenge, then reverse transcribed, sequenced, and compared to sequence data from the SHIV inoculum. We focused on the SIV RT and IN coding regions, the two targets for cART components PMPA/FTC and raltegravir, respectively. In Group I and II animals, no resistance mutations were observed prior to cART (Supplementary Table 1), and the subsequently durable and sustained suppression in these animals is a strong indicator that no drug resistance mutations emerged (although this was not confirmed as viral loads became too low for deep sequencing). Consistent with our hypothesis, we detected multiple known drug resistance mutations in Group III animals following cART initiation (Supplementary Table 1 and Figure 2). Pol N155H, a raltegravir resistance mutation [17–19], was detected within 3–9 weeks of cART initiation in the Group III animals (Figure 2A). In A11202, this mutation had grown to saturation when the animal was necropsied 38 weeks post-SHIV challenge. A11205 was euthanized at 27 weeks post-SHIV challenge due to persistent thrombocytopenia and anemia, at which point the N155H mutation constituted 71% of the total population of SHIV Pol sequences. As was observed with A11202, this mutation was also trending towards saturation. The PMPA resistance mutation, K65R in SIV RT [20–22], was also detected in animal A11202 within 15 weeks of cART initiation (Supplementary Table 1 and Figure 2B). Hence, selection of cART-resistant SHIV viruses appears to be facilitated in post-transplant animals.

Plasma cART levels in post-transplant animals are comparable to controls

The Group II and III transplanted animals received a myeloablative conditioning regimen consisting of 1020 cGy total body irradiation (TBI), a dose associated with damage to the gut [23, 24]. This may interfere with absorption and bioavailability of the orally dosed cART component, raltegravir, facilitating selection of drug-resistant viral variants. We therefore used mass spectrometry to test whether PT animals (Group III) had lower circulating levels of cART compared to animals that were transplant-naïve at the time of cART initiation (Groups I–II). We measured plasma levels of each drug 1–2 weeks and 13–20 weeks following cART initiation (Supplementary Figure 1A). At 1–2 weeks post-cART, plasma levels of tenofovir ranged between 13.7 and 74.8 ng/mL in Groups I and II and between 19.2 and 37.3 ng/mL in Group III animals (Figure S1B). Similarly, plasma concentrations of FTC in Group III animals (83.5 ng/mL and 83.0 ng/mL) fell within the range of 29.0–212.0 ng/mL found in Group I–II animals (Figure S1C). Most importantly, the orally dosed component, raltegravir, was also comparable: Group III animals had 139.0 and 771.0 ng/mL, both within the range of 32.6–1480 ng/mL in Groups I–II (Figure S1D). At 13–20 weeks, cART levels in each animal generally varied by less than 3-fold from their

levels 1–2 weeks post-cART, with the exception of Group II animal Z09144, which displayed a drastic increase in plasma concentrations of tenofovir and FTC (Figure S1B). Although drug resistance mutations were detected in Group III at this time point (Figure 2), their plasma tenofovir and FTC concentrations were still within the range detected in Group I and II controls (Figure S1B–C), while plasma raltegravir concentrations were higher than those in Group I and II (Figure S1D). Thus, cART resistance mutations in PT animals are unlikely to have arisen as a result of decreased plasma bioavailability.

Infection of myeloid subsets in post-transplant animals is comparable to controls

We tested two additional models that could explain why the Group III animals developed cART-refractory plasma viremia. First, we reasoned that the combination of sustained peak plasma viremia (Figure 1) and low baseline CD4+ T-cell counts (Figure 3) could have facilitated infection of peripheral blood CD4+ myeloid cells, which could serve as drug sanctuaries [25–27]. No significant differences in average monocyte counts were found in any animal during the course of study except for an elevation in Group III animal A11202 between 6 and 12 weeks post-SHIV challenge (Supplementary Figure 2A–C). However, the ratio of monocytes to CD4+ T-cells was significantly elevated in Group III animals relative to Group I and II controls prior to ($p<0.001$) and following ($p = 0.003$) SHIV challenge (Supplementary Figure 2D–F). To test the hypothesis that an elevated ratio of monocytes to CD4+ T-cells is associated with increased infection of monocytic and other myeloid subsets, we measured total SHIV DNA in peripheral lymphoid (CD3+) vs. myeloid (CD14+) cells following sequential magnetic bead-based sorting (Supplementary Figure 3). The SHIV viral DNA load in CD14+ cells, which on average contained less than 4% CD3+ contamination (Figure S3A), was comparable across all three groups of animals (Figure S3B), as was the viral DNA load in CD3+ cells (Figure S3C). Hence, the ratio of SHIV DNA+ CD14+ cells to SHIV DNA+ CD3+ cells was not significantly different ($p=0.26$) between Group III and Groups I–II (Figure S3D). These data suggest that SHIV DNA+ peripheral blood cells in PT animals were not overtly skewed towards a monocytic (CD14+) lineage.

Marked depletion of total and naïve CD4+ and naïve CD8+ T-cells is associated with drug resistance

Our second model to explain development of cART-resistant plasma viremia in post-transplant animals was a loss of T- and B-cell-dependent restriction of infection during the acute phase, presumably due to insufficient hematopoietic reconstitution post-HSCT [28–30]. Group I and II animals exhibited a mild decline of CD4+ cells during acute infection, with two animals in Groups I–II (Group I: Z09087, Group II: Z09144) declining further over 6 months of infection prior to cART initiation. CD4+ T-cell counts gradually increased upon initiation of cART in all animals. Group II animals experienced a drop to <100 cells/μL following total body irradiation (TBI) during HSCT at week 53–56 (Figure 3A) and then gradually recovered. Group III (PT) animals had significantly lower pre-SHIV CD4+ T-cell counts than Groups I–II ($p<0.0001$; Figure 3B), decreased further in the first 9–10 weeks post-SHIV challenge, prior to initiation of cART (Figure 3C) but then recovered at a similar rate upon initiation of cART (Figure 3A). Analogous, but less striking trends were observed in peripheral blood CD8+ T-cell counts (Figure 3D–F). A marked depletion of peripheral blood naïve CD4+ and CD8+ T-cells was also noted in Group III prior to SHIV challenge

and cART (Figure S4B–S4C). Similar to total CD4+ T-cells, naïve subsets remained suppressed until initiation of cART in these animals. By contrast, central and effector memory T-cell counts in Group III animals were more difficult to distinguish from Group I–II controls (Figure S4D–S4G). Depletion of CD4+ and CD4+CCR5+ T-cells in upper and lower GI was comparable across all Groups (Supplementary Figure S4H–S4K), as was depletion of peripheral blood CD4+CCR5+ cells (Figure S4A). Although we did not observe statistically significant differences in these counts, we did observe an unexpectedly rapid rebound of CD4+CCR5+ T-cells in each compartment following cART initiation in Group III. Taken together, these data indicate that post-transplant animals' total and naive CD4+, and naïve CD8+ T-cell counts are suppressed due to TBI, remain suppressed during acute SHIV infection, and rebound following cART, despite persistent plasma viremia.

Drastic reduction in SHIV-specific antibody production in post-transplant animals

To assess B-cell function during acute SHIV infection in Groups I–III, we longitudinally measured production of anti-SHIV antibodies: those against SIVmac239, the backbone of the env-SHIV virus used (Figure 4A), and against a heterologous HIV envelope, SF162 (Figure 4B). Anti-SHIV antibody production in Groups I and II was comparable: production was first detected within 5 weeks of SHIV challenge, increased to 4–5 logs prior to cART initiation, and decreased by approximately 1 log following cART (Figure 4A,B). In contrast, anti-SIV antibodies were very low in Group III animals: they were not detected in A11202 until 25 weeks post-SHIV challenge (15 weeks post-cART), and remained 2–3 logs below Groups I and II. Anti-SIV antibodies were initially detected early in Group III animal A11205 but fluctuated above and below the limit of detection (Figure 4A). Anti-HIV Env antibodies were not detected in A11202 until week 25 post-infection, while levels in A11205 remained near the limit of detection throughout the course of study (Figure 4B). Importantly, CD20+ B-cell levels were roughly comparable in all three groups throughout the study, with the exception of the transient depletion observed in Group II following TBI, and a slight decrease in Group III animal A11202 prior to initiation of cART at week 10 post-infection (Figure 4C). These results suggest that Group III animals lack an acute antibody response following SHIV challenge, which is independent of CD20+ B-cell levels.

Discussion

We demonstrate that post-transplant animals undergoing autologous HSCT-mediated gene therapy 100 days prior to SHIV challenge are subject to an aggressive acute phase of infection, rapid resistance to cART therapy, and poorer prognosis (Figures 1 and 2). Our data suggest that accrual of cART resistance mutations is neither a function of suboptimal cART bioavailability (Figure S1), nor of an augmented repertoire of infection-susceptible cells in peripheral blood (Figure S3). Rather, we observed decreased T-cell counts in post-transplant animals prior to infection, which was further exacerbated during the initial phase of infection (Figure 3). Although B-cell counts in these animals were unchanged relative to the impact on T-cells, production of SHIV-specific antibodies was highly impaired (Figure 4). These findings are most consistent with a model in which immune cell counts and functionality, drastically reduced following TBI, are only partially restored at the time of SHIV challenge. The impaired immune system appears to be unable to restrict infection

during the acute phase, resulting in sustained peak viremia, facilitating selection for drug-resistant mutants upon cART initiation, and ultimately accelerating disease progression (Figure 5).

These data reinforce recent findings from our group and others [13, 31], that autologous HSCT, including myeloablative TBI, is safe and feasible in infected, stably suppressed animals (Figure 1B–C). Conversely, PT animals (Figure 1D) exhibited a more pathogenic course of infection following SHIV challenge, a finding that is relevant to clinical analytical treatment interruption (ATI) studies. Our data is consistent with recent findings from Henrich et al. [6], in which one of the two HIV+ Boston patients undergoing reduced-intensity conditioning and allogeneic stem cell transplantation developed cART resistance following ATI. Importantly, the Boston patient's resistance arose despite the fact that ATI was over two years removed from HSCT; the fact that this patient remained on immunosuppressive therapy suggests that our observations may extend far beyond acute (100 days) recovery post-HSCT. It remains to be determined what complicating factors may have also contributed to cART resistance in this patient, for example, cART adherence anomalies before or after HSCT, or ongoing immunosuppressive therapy and GVHD. In stark contrast, the Berlin patient ceased cART therapy concurrent with the first of two rounds of myeloablative conditioning, yet remains free of detectable replication-competent virus over 8 years later [4, 32]. We are currently investigating the contributions made by infusion of infection-resistant cells to better model the clinical course of the Berlin patient. In these experiments, animals undergoing a 200-day recovery post-transplant exhibit a more prototypical course of SHIV infection, as compared to Group III animals in the present study that recovered for 100 days (manuscripts in preparation). These findings suggest that the period between 100 and 200 days post-transplant is a critical recovery window, during which the host immune system recovers sufficiently to respond to SHIV challenge. Our ongoing *de novo* infection experiments, as well as experiments involving ATI in infected and cART-suppressed animals, now include a standard 200-day recovery post-transplant.

Myeloablative conditioning regimens such as TBI may augment replication-competent viral reservoirs in two ways. First, residual tissue damage following TBI may impair cART uptake. Our data suggest that plasma drug levels are comparable in post-transplant animals, relative to transplant-naïve controls (Figure S1). These data leave open the possibility that antiretroviral (ARV) uptake from plasma is impaired in select tissues, leading to establishment of novel drug sanctuaries and persistent SHIV replication. Second, TBI may also have accelerated seeding of infection in tissues such as the central nervous system (CNS), since TBI and associated inflammation are known to permeabilize the blood brain barrier (BBB; [33–35]). TBI-dependent permeabilization of the BBB could facilitate passage of replication-competent virus into the CNS. Following BBB repair, when cART delivery to the CNS may be impeded, this enhanced viral reservoir would represent a significant barrier to cART-mediated suppression [36]. Together, alterations in ARV drug biodistribution and tissue exposure to infectious virus following HSCT could explain why we observed rebound of peripheral blood CD4+ T-cells following cART initiation, despite incomplete suppression of plasma viremia. Despite normal plasma levels of ARVs and full protection of circulating CD4+ T-cells, cART-refractory and/or SHIV hyper-penetrant tissues may have represented

the source of high circulating levels of virus. We are currently mapping the animal-wide and cell type-specific biodistribution of ARVs, SHIV RNA, and SHIV DNA to identify anomalies in experimental groups such as post-transplant animals. Although techniques to measure intracellular cART concentrations on a per-cell basis are still in their infancy, we believe that understanding the relative distribution of virus and cART in our model will allow us to characterize the overlap between sites of active viral replication and drug exclusion. Such detailed mapping will allow for the detection of alterations in post-transplant animals and HIV^+ gene therapy patients.

CCR5-tropic SHIVs, as used in this study, manifest acute pathogenesis primarily in secondary lymphoid tissues like the GI tract rather than peripheral blood, due to the relative numbers of $CD4^+CCR5^+$ target cells in these compartments [16, 37–39]. Notably, B-cell defects have also been observed at these tissue sites [40–42]. We observed an unexpectedly dramatic loss of CD4+ T-cells in the peripheral blood in the post-transplant animals following SHIV challenge, which rebounded rapidly following initiation of cART (Figure 3). Similar, less striking trends were observed in the GI tract (Figure S4). Paradoxically, rebound in $CD4^+CCR5^+$ counts following cART occurred despite ongoing viral replication in post-transplant animals. We have no evidence to suggest that these rebounding cells are refractory to SHIV infection. Rather, these results are consistent with our recent finding that HSCT-dependent mechanisms upregulate CCR5 expression on circulating T-cells [13]. We hypothesize that *de novo* expression of CCR5 at the surface of previously $CD4^+CCR5^-$ cells replenishes the pool of infection-susceptible targets, generating target cells at a greater rate than they are eliminated by ongoing infection. The balance between generation and killing of $CD4^+CCR5^+$ cells is further complicated by the decrease in naïve T-cells we observe (Figure S4B–C), which may skew infection towards effector memory T-cells (Figure S4F–G). We are currently investigating impairment of peripheral blood T-cell function in post-transplant animals, and are also examining the role of other regulatory cells in the periphery, such as myeloid-derived suppressor cells [43, 44]. A better understanding of the effects of HSCT on CCR5 expression by $CD4^+$ cells will be required in order to generate effective CCR5-based antiviral therapies.

Finally, our findings are consistent with recent work from Micci et al. [45] in which experimental CD4 depletion followed by SIVmac251 challenge resulted in sustained high plasma viremia. Interestingly, the authors observed massive inflammation and infection of myeloid subsets in their animals. We similarly postulate that myeloid subsets might be at increased susceptibility for infection in post-transplant animals. Although we did not observe a significant enrichment of SHIV DNA+ CD14+ cells either prior to or following initiation of cART (Figure S3), this analysis was limited to peripheral blood, whereas Micci et al. observed dramatic effects in lymph nodes, gut, and CNS. It will be intriguing to compare the effects of TBI, which our data and past work shows is broadly lymphotoxic [46], to targeted CD4 depletion. Comparing these two models may reveal TBI-sensitive cellular subsets in blood and tissue whose function is required for gene therapy-mediated protection during ATI.

To summarize, we observed that immune-compromised animals exhibited sustained peak plasma viremia following SHIV challenge and were at increased risk for development of

cART resistance mutations following cART initiation. These effects were associated with low levels of total and naïve CD4+ and naïve CD8+ T-cells, and deficiencies in the production of anti-SHIV antibodies. These results begin to shed light on the complex, multifactorial immune deficiency that exists following myeloablative HSCT, and underscore the need for exhaustive measurement of immune homeostasis in the context of gene therapy-mediated HIV cure trials.

Supplementary Material

Refer to Web version on PubMed Central for supplementary material.

Acknowledgments

Grant support: This work was supported by grants from the National Institutes of Health, Bethesda, MD: P30 AI050410; R01 AI111891; U19 AI096113; P01 AI097100; R01 HL116217; R01 AI080326. HPK is a Markey Molecular Medicine Investigator and received support as the inaugural recipient of the José Carreras/E. Donnall Thomas Endowed Chair for Cancer Research.

References

1. Hutter G, Nowak D, Mossner M, Ganepola S, Mussig A, Allers K, et al. Long-term control of HIV by CCR5 Delta32/Delta32 stem-cell transplantation. N Engl J Med. 2009; 360(7):692–698. [PubMed: 19213682]
2. Allers K, Hutter G, Hofmann J, Loddenkemper C, Rieger K, Thiel E, et al. Evidence for the cure of HIV infection by CCR5Δ32/Δ32 stem cell transplantation. Blood. 2011; 117(10):2791–2799. [PubMed: 21148083]
3. Hutter G, Thiel E. Allogeneic transplantation of CCR5-deficient progenitor cells in a patient with HIV infection: an update after 3 years and the search for patient no. 2. AIDS. 2011; 25(2):273–274. [PubMed: 21173593]
4. Yukl SA, Boritz E, Busch M, Bentsen C, Chun TW, Douek D, et al. Challenges in detecting HIV persistence during potentially curative interventions: a study of the Berlin patient. PLoS Pathogens. 2013; 9(5):e1003347. [PubMed: 23671416]
5. Henrich TJ, Hu Z, Li JZ, Sciaranghella G, Busch MP, Keating SM, et al. Long-term reduction in peripheral blood HIV type 1 reservoirs following reduced-intensity conditioning allogeneic stem cell transplantation. J Infect Dis. 2013; 207(11):1694–1702. [PubMed: 23460751]
6. Henrich TJ, Hanhauser E, Marty FM, Sirignano MN, Keating S, Lee TH, et al. Antiretroviral-free HIV-1 remission and viral rebound after allogeneic stem cell transplantation: report of 2 cases. Ann Intern Med. 2014; 161(5):319–327. [PubMed: 25047577]
7. Beard BC, Trobridge GD, Ironside C, McCune JS, Adair JE, Kiem H-P. Efficient and stable MGMT-mediated selection of long-term repopulating stem cells in nonhuman primates. J Clin Invest. 2010; 120(7):2345–2354. [PubMed: 20551514]
8. Chong JJ, Yang X, Don CW, Minami E, Liu YW, Weyers JJ, et al. Human embryonic-stem-cell-derived cardiomyocytes regenerate non-human primate hearts (Letter). Nature. 2014; 510(7504): 273–277. [PubMed: 24776797]
9. Kiem HP, Arumugam PI, Burtner CR, Fox C, Beard BC, Dexheimer P, et al. Pigtailed macaques as a model to study long-term safety of lentivirus vector-mediated gene therapy for hemoglobinopathies. 9999.
10. Younan PM, Polacino P, Kowalski JP, Peterson CW, Maurice NJ, Williams NP, et al. Positive selection of mC46-expressing CD4+ T cells and maintenance of virus specific immunity in a primate AIDS model. Blood. 2013; 122(2):179–187. [PubMed: 23719296]
11. Peterson CW, Younan P, Polacino PS, Maurice NJ, Miller HW, Prlic M, et al. Robust suppression of env-SHIV viremia in Macaca nemestrina by 3-drug ART is independent of timing of initiation

during chronic infection. Journal of Medical Primatology. 2013; 42(5):237–246. [PubMed: 24025078]

12. Matrajt L, Younan PM, Kiem HP, Schiffer JT. The majority of CD4+ T-cell depletion during acute simian-human immunodeficiency virus SHIV89.6P infection occurs in uninfected cells. J Virol. 2014; 88(6):3202–3212. [PubMed: 24390339]
13. Younan PM, Peterson CW, Polacino P, Kowalski JP, Obenza W, Miller HW, et al. Lentivirus mediated gene transfer in hematopoietic stem cells is impaired in SHIV-infected, ART-treated nonhuman primates. Mol Ther. 2015 Epub ahead of print. 10.1038/mt.2015.19
14. Trobridge GD, Beard BC, Gooch C, Wohlfahrt M, Olsen P, Fletcher J, et al. Efficient transduction of pigtailed macaque hemtopoietic repopulating cells with HIV-based lentiviral vectors. Blood. 2008; 111(12):5537–5543. [PubMed: 18388180]
15. Song RJ, Chenine AL, Rasmussen RA, Ruprecht CR, Mirshahidi S, Grisson RD, et al. Molecularly cloned SHIV-1157ipd3N4: a highly replication- competent, mucosally transmissible R5 simian-human immunodeficiency virus encoding HIV clade C Env. J Virol. 2006; 80(17):8729–8738. [PubMed: 16912320]
16. Ho O, Larsen K, Polacino P, Li Y, Anderson D, Song R, et al. Pathogenic infection of Macaca nemestrina with a CCR5-tropic subtype-C simian-human immunodeficiency virus. Retrovirology. 2009; 6:65. (note: no issue number). [PubMed: 19602283]
17. Cooper DA, Steigbigel RT, Gatell JM, Rockstroh JK, Katlama C, Yeni P, et al. Subgroup and resistance analyses of raltegravir for resistant HIV-1 infection. N Engl J Med. 2008; 359(4):355–365. [PubMed: 18650513]
18. Malet I, Delelis O, Soulie C, Wirden M, Tchertanov L, Mottaz P, et al. Quasispecies variant dynamics during emergence of resistance to raltegravir in HIV-1-infected patients. J Antimicrob Chemother. 2009; 63(4):795–804. [PubMed: 19221102]
19. Hassounah SA, Mesplede T, Quashie PK, Oliveira M, Sandstrom PA, Wainberg MA. Effect of HIV-1 integrase resistance mutations when introduced into SIVmac239 on susceptibility to integrase strand transfer inhibitors. J Virol. 2014; 88(17):9683–9692. [PubMed: 24920794]
20. Miller MD, Margot NA, Hertogs K, Larder B, Miller V. Antiviral activity of tenofovir (PMPA) against nucleoside-resistant clinical HIV samples. Nucleosides, Nucleotides & Nucleic Acids. 2001; 20(4–7):1025–1028.
21. Ruane PJ, Luber AD. K65R-associated virologic failure in HIV-infected patients receiving tenofovir-containing triple nucleoside/nucleotide reverse transcriptase inhibitor regimens (Review). Medscape General Medicine. 2004; 6(2):31. [PubMed: 15266257]
22. Van Rompay KK, Trott KA, Jayashankar K, Geng Y, LaBranche CC, Johnson JA, et al. Prolonged tenofovir treatment of macaques infected with K65R reverse transcriptase mutants of SIV results in the development of antiviral immune responses that control virus replication after drug withdrawal. Retrovirology. 2012; 9:57. [PubMed: 22805180]
23. Johansson JE, Brune M, Ekman T. The gut mucosa barrier is preserved during allogeneic, haemopoietic stem cell transplantation with reduced intensity conditioning. Bone Marrow Transplant. 2001; 28(8):737–742. [PubMed: 11781624]
24. Asano S. Current status of hematopoietic stem cell transplantation for acute radiation syndromes (Review). Int J Hematol. 2012; 95(3):227–231. [PubMed: 22382644]
25. Pollicita M, Surdo M, Di Santo F, Cortese MF, Fabeni L, Fedele V, et al. Comparative replication capacity of raltegravir-resistant strains and antiviral activity of the new-generation integrase inhibitor dolutegravir in human primary macrophages and lymphocytes. J Antimicrob Chemother. 2014; 69(9):2412–2419. [PubMed: 24860155]
26. Koppensteiner H, Brack-Werner R, Schindler M. Macrophages and their relevance in Human Immunodeficiency Virus Type I infection (Review). Retrovirology. 2012; 9:82. [PubMed: 23035819]
27. Cory TJ, Schacker TW, Stevenson M, Fletcher CV. Overcoming pharmacologic sanctuaries (Review). Current Opinion in HIV & AIDS. 2013; 8(3):190–195. [PubMed: 23454865]
28. Nishimura Y, Martin MA. The acute HIV infection: implications for intervention, prevention and development of an effective AIDS vaccine (Review). Current Opinion in Virology. 2011; 1(3): 204–210. [PubMed: 21909345]

29. Mouquet H. Antibody B cell responses in HIV-1 infection. Trends Immunol. 2014 Epub ahead of print 2014 Sept 15. 10.1016/j.it.2014.08.007
30. Borrow P. Innate immunity in acute HIV-1 infection (Review). Current Opinion in HIV & AIDS. 2011; 6(5):353–363. [PubMed: 21734567]
31. Mavigner M, Watkins B, Lawson B, Lee ST, Chahroudi A, Kean L, et al. Persistence of virus reservoirs in ART-treated SHIV-infected rhesus macaques after autologous hematopoietic stem cell transplant. PLoS Pathogens. 2014; 10(9):e1004406. [PubMed: 25254512]
32. Hutter G, Ganepola S. Eradication of HIV by transplantation of CCR5-deficient hematopoietic stem cells. The Scientific World Journal. 2011; 11:1068–1076. [PubMed: 21552772]
33. van Vulpen M, Kal HB, Taphoorn MJ, El-Sharouni SY. Changes in blood-brain barrier permeability induced by radiotherapy: implications for timing of chemotherapy? (Review). Oncology Reports. 2002; 9(4):683–688. [PubMed: 12066192]
34. Lopez-Ramirez MA, Wu D, Pryce G, Simpson JE, Reijerkerk A, King-Robson J, et al. MicroRNA-155 negatively affects blood-brain barrier function during neuroinflammation. FASEB J. 2014; 28(6):2551–2565. [PubMed: 24604078]
35. Minagar A, Alexander JS. Blood-brain barrier disruption in multiple sclerosis (Review). Multiple Sclerosis. 2003; 9(6):540–549. [PubMed: 14664465]
36. Yilmaz A, Price RW, Gisslen M. Antiretroviral drug treatment of CNS HIV-1 infection (Review). J Antimicrob Chemother. 2012; 67(2):299–311. [PubMed: 22160207]
37. Harouse JM, Gettie A, Tan RC, Blanchard J, Cheng-Mayer C. Distinct pathogenic sequela in rhesus macaques infected with CCR5 or CXCR4 utilizing SHIVs. Science. 1999; 284(5415):816–819. [PubMed: 10221916]
38. Pandrea I, Apetrei C, Gordon S, Barbercheck J, Dufour J, Bohm R, et al. Paucity of CD4+CCR5+ T cells is a typical feature of natural SIV hosts. Blood. 2007; 109(3):1069–1076. [PubMed: 17003371]
39. Ling B, Mohan M, Lackner AA, Green LC, Marx PA, Doyle LA, et al. The large intestine as a major reservoir for simian immunodeficiency virus in macaques with long-term, nonprogressing infection. J Infect Dis. 2010; 202(12):1846–1854. [PubMed: 21050120]
40. Dykhuizen M, Mitchen JL, Montefiori DC, Thomson J, Acker L, Lardy H, et al. Determinants of disease in the simian immunodeficiency virus-infected rhesus macaque: characterizing animals with low antibody responses and rapid progression. J Gen Virol. 1998; 79(Pt 10):2461–2467. [PubMed: 9780052]
41. Levesque MC, Moody MA, Hwang KK, Marshall DJ, Whitesides JF, Amos JD, et al. Polyclonal B cell differentiation and loss of gastrointestinal tract germinal centers in the earliest stages of HIV-1 infection. PLoS Medicine. 2009; 6(7):e1000107. [PubMed: 19582166]
42. Xu H, Wang X, Veazey RS. Mucosal immunology of HIV infection (Review). Immunol Rev. 2013; 254(1):10–33. [PubMed: 23772612]
43. Macatangay BJ, Landay AL, Rinaldo CR. MDSC: a new player in HIV immunopathogenesis. AIDS. 2012; 26(12):1567–1569. [PubMed: 22810370]
44. Sui Y, Hogg A, Wang Y, Frey B, Yu H, Xia Z, et al. Vaccine-induced myeloid cell population dampens protective immunity to SIV. J Clin Invest. 2014; 124(6):2538–2549. [PubMed: 24837435]
45. Micci L, Alvarez X, Iriele RI, Ortiz AM, Ryan ES, McGary CS, et al. CD4 depletion in SIV-infected macaques results in macrophage and microglia infection with rapid turnover of infected cells. PLoS Pathogens. 2014; 10(10):e1004467. [PubMed: 25356757]
46. Heylmann D, Rodel F, Kindler T, Kaina B. Radiation sensitivity of human and murine peripheral blood lymphocytes, stem and progenitor cells (Review). Biochim Biophys Acta. 2014; 1846(1): 121–129. [PubMed: 24797212]
47. Polacino P, Cleveland B, Zhu Y, Kimata JT, Overbaugh J, Anderson D, et al. Immunogenicity and protective efficacy of Gag/Pol/Env vaccines derived from temporal isolates of SIVmne against cognate virus challenge. Journal of Medical Primatology. 2007; 36(4–5):254–265. [PubMed: 17669214]

48. Hu SL, Zarling JM, Chinn J, Travis BM, Moran PA, Sias J, et al. Protection of macaques against simian AIDS by immunization with a recombinant vaccinia virus expressing the envelope glycoproteins of simian type D retrovirus. PNAS. 1989; 86(18):7213–7217. [PubMed: 2550935]

49. Rodrigo AG, Goracke PC, Rowhanian K, Mullins JI. Quantitation of target molecules from polymerase chain reaction-based limiting dilution assays. AIDS Res Hum Retroviruses. 1997; 13(9):737–742. [PubMed: 9171217]

50. Hofmann-Lehmann R, Swenerton RK, Liska V, Leutenegger CM, Lutz H, McClure HM, et al. Sensitive and robust one-tube real-time reverse transcriptase-polymerase chain reaction to quantify SIV RNA load: comparison of one- versus two-enzyme systems. AIDS Res Hum Retroviruses. 2000; 16(13):1247–1257. [PubMed: 10957722]

51. Limaye AP, Huang M-L, Leisenring W, Stensland L, Corey L, Boeckh M. Cytomegalovirus (CMV) DNA load in plasma for the diagnosis of CMV disease before engraftment in hematopoietic stem-cell transplant recipients. J Infect Dis. 2001; 183:377–382. [PubMed: 11133368]

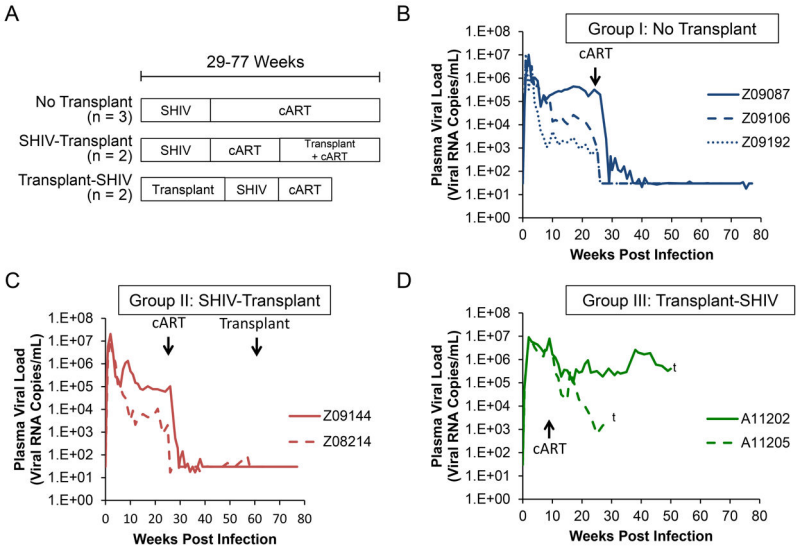

Figure 1. cART-resistant SHIV plasma viremia is observed in post-transplant *M. nemestrina*

A) Longitudinal plasma viral loads were measured in 3 untransplanted animals ("No transplant"), 2 animals infected with SHIV and then transplanted ("SHIV-transplant"), and two animals transplanted and then infected with SHIV ("transplant-SHIV"). **B–D**) Viral loads over time in each of the three groups. Crosses represent necropsy for A11202 and A11205 (Group III).

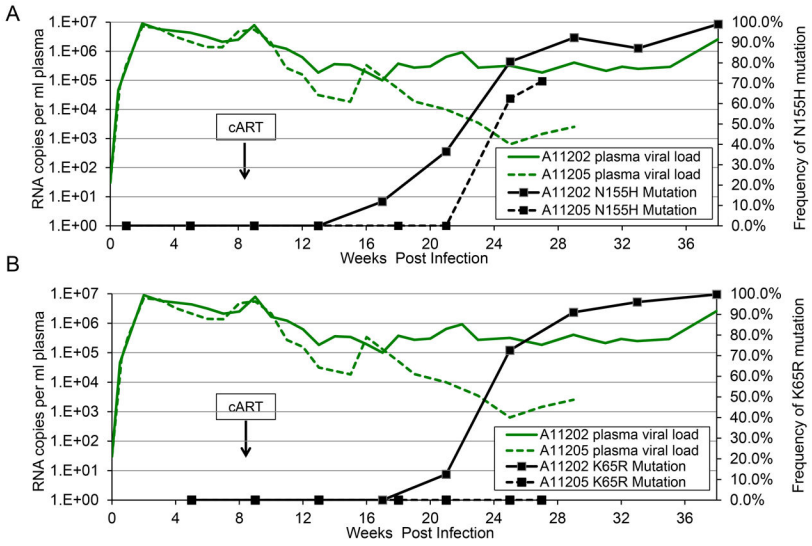

Figure 2. Detection of drug resistance mutations in SHIV integrase and reverse transcriptase in post-transplant animals

Total RNA was extracted from plasma from Post-transplant animals A11202 (solid lines) and A11205 (dotted lines) and subjected to Illumina MiSeq deep sequencing at SHIV integrase (**A**) and reverse transcriptase **(B)**. Green lines represent plasma viral loads. Black boxes represent frequency of sequencing reads containing the indicated mutation. Arrows denote initiation of cART at 9–10 weeks post-challenge.

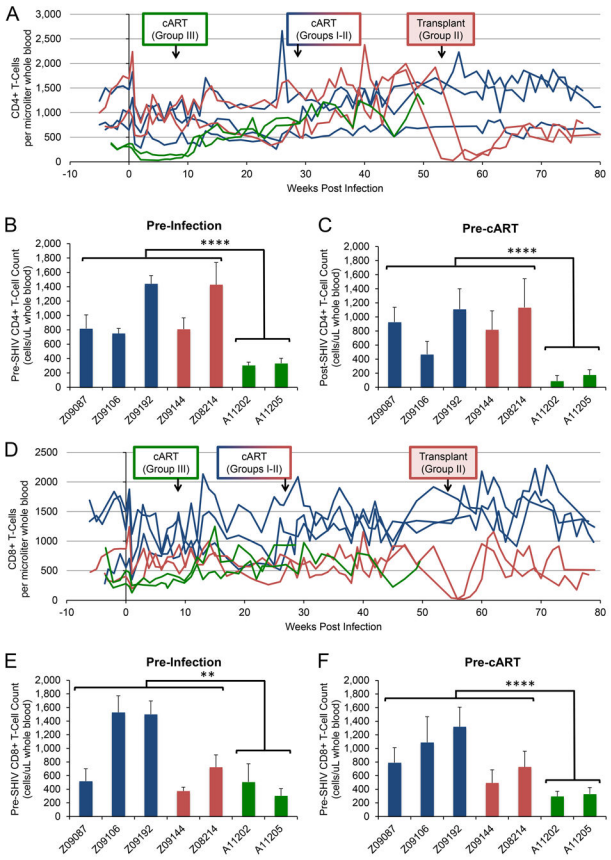

Figure 3. Peripheral blood T-cell counts are suppressed prior to SHIV challenge in post-transplant animals, but recover following initiation of cART

Flow cytometry was used to longitudinally measure T-cell counts in peripheral blood from no transplant (blue), SHIV-transplant (red), and transplant-SHIV (green) animals. Arrows indicate time of cART initiation and autologous transplant, where applicable, for each group. **A**) $CD4^+$ T-cell counts/μL over the course of SHIV infection in each animal. **B**) Average $CD4^+$ T-cell counts over 4–6 weeks prior to SHIV challenge. **C**) Average $CD4^+$ T-cell counts over 9–10 weeks post-challenge, prior to Group III animals initiating cART. **D**) $CD8^+$ T-cell counts/μL were measured longitudinally as in A). **E**) Average $CD8^+$ T-cell counts over 4–6 weeks prior to SHIV challenge. **F**) Average $CD8^+$ T- cell counts over 9–10 weeks post-challenge, prior to Group III animals initiating cART. Error bars represent standard deviations between weekly measurements. Statistical significance between collective measurements from Groups I–II and Group III was measured by single-tailed Student's t-test. ** represents $p < 0.01$, and **** represents $p < 0.0001$.

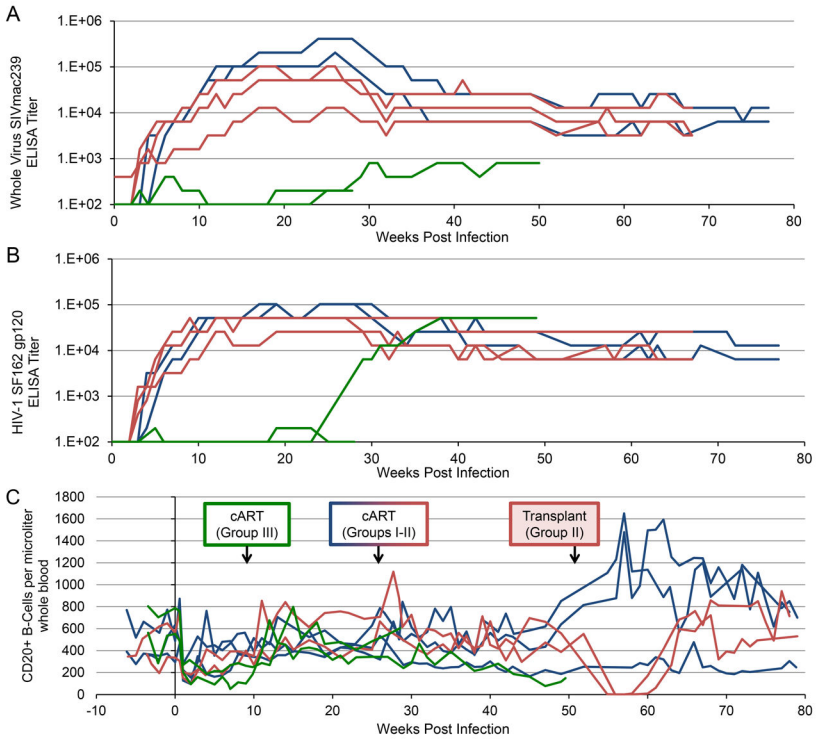

Figure 4. Post-transplant animals display significant impairment in production of anti-SHIV antibodies, despite comparable CD20$^+$ B-cell counts

ELISA was used to measure the serum titer of antibodies specific for SIVmac239 (**A**) or HIV-1 SF162 Env (**B**) from no transplant (blue), SHIV-transplant (red), and transplant-SHIV (green) animals. Titer was calculated as the reciprocal of the highest serum dilution that resulted in an optical density reading greater than the average values obtained with negative macaque sera plus three standard deviations. **C**) CD20$^+$ B-cell counts per μL in peripheral blood were measured by flow cytometry. Arrows indicate time of cART initiation and autologous transplant, where applicable, for each group.

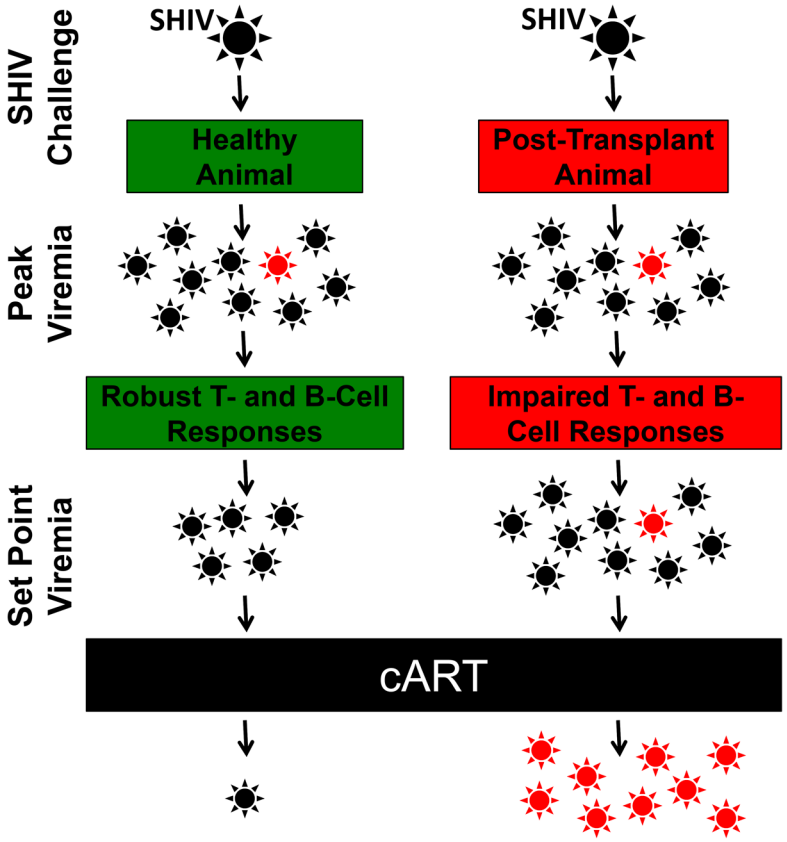

Figure 5. Model for cART resistance in post-transplant animals

Following SHIV challenge, healthy animals and post-transplant animals stochastically generate equivalent numbers of cART-resistant mutants (red). In healthy animals, T- and B-cell responses and decreased viral fitness both restrict propagation of these mutants. In contrast, post-transplant animals' impaired T- and B-cell repertoire limit viral restriction during the transition to set point viremia, increasing the likelihood that mutants will persist in sufficient numbers to undergo positive selection following initiation of cART.